Environment International 198 (2025) 109424

Contents lists available at ScienceDirect

Environment International

journal homepage: www.elsevier.com/locate/envint

Full length article

Oxidative potential of urban $PM_{2.5}$ in relation to chemical composition: Importance of fossil driven sources

Joo-Ae Kim [a,b,1], Seulki Jeong [c,d,1], Saehee Lim [e], Yongjoo Choi [f], Hyomin Kim [a], Meehye Lee [a,*]

[a] Department of Earth and Environmental Science, Korea University, 145 Anam-ro, Seongbuk-gu, Seoul 02841, Republic of Korea
[b] The Institute of Basic Science, Korea University, 145 Anam-ro, Seongbuk-gu, Seoul 02841, Republic of Korea
[c] Metropolitan Seoul Center, Korea Basic Science Institute, 145 Anam-ro, Seongbuk-gu, Seoul 02841, Republic of Korea
[d] Department of Environment & Energy, Sejong University, 209 Neungdong-ro, Gwangjin-gu, Seoul 05006, Republic of Korea
[e] Department of Environment and IT Engineering, Chungnam National University, Daejeon 34134, Republic of Kore
[f] Department of Environmental Science, Hankuk University of Foreign Studies, 81 Oedae-ro, Mohyeon-myeon, Cheoin-gu, Yongin-si, Gyeonggi-do 17035, Republic of Korea

ARTICLE INFO

Editor: Dr. Xavier Querol

Keywords:
$PM_{2.5}$
Oxidative potential, DTT assay
Fossil fuel
Stable isotopic ratio

ABSTRACT

For a comprehensive evaluation of the key factors determining the oxidative potential (OP) of $PM_{2.5}$, 75 samples of $PM_{2.5}$ were collected in urban Seoul, South Korea, during 2019–2021, and dithiothreitol consumption (DTTv) was measured using a DTT assay, coupled with an analysis of major constituents and stable isotope ratios of $PM_{2.5}$. For the entire sample set, the mean DTTv value was 0.58 ± 0.48 nmol m^{-3} min^{-1} for $PM_{2.5}$ of 29.1 ± 12.2. DTTv exhibited a general dependence on of $PM_{2.5}$ concentrations and major constituents, including NO_3^-, SO_4^{2-}, NH_4^+, and organic carbon (OC). Specifically, NO_3^- and NH_4^+ demonstrated the most robust correlation with DTTv during the cold season, whereas only elemental carbon (EC) showed a significant correlation with DTTv in the warm season. The $\delta^{13}C$ of total carbon (TC) and $\delta^{15}N$ of total nitrogen (TN) displayed an inverse correlation concerning DTT activities, suggesting the significant contribution from solid fossil fuels and biomass burning to the oxidative potential of $PM_{2.5}$, particularly during the cold season when $PM_{2.5}$ was notably high. In contrast, vehicle emissions were found to influence DTTv even at low $PM_{2.5}$ levels in warm seasons. This study provides insights into the intricate dynamics influencing the oxidative potential of $PM_{2.5}$.

1. Introduction

Atmospheric fine aerosols affect not only human health on a local scale but also climate change on a global scale. Air pollution has been reported to be associated with over 8 million premature deaths worldwide (WHO, 2020). Epidemiological studies have shown that exposure to particulate matter (PM) can lead to short- and long-term health effects, including respiratory problems, cardiovascular disorders, mental health impairments, and carcinogenic diseases (Fajersztajn et al., 2013; Pascal et al., 2013; Peters et al., 2006; Sint et al.,2008). Numerous studies investigated the quantitative health effects of PM, and oxidative stress was suggested as an important mechanism through which PM leads to adverse health effects. Oxidative stress, a biological imbalance wherein the generation of reactive oxygen species (ROS) or free radicals exceed antioxidant defenses, can induce oxidative damage, and eventually lead to various adverse health effects (Cho et al., 2005; Patel et al., 2022; Pizzino et al., 2017). Oxidative potential was proposed as a versatile indicator for the evaluation of the ability of PM to generate ROS, which eventually indices PM toxicity.

Several chemical and biological methods have been developed to measure the oxidative potential. The dithiothreitol (DTT) assay, which acts as a surrogate for cellular reductants, is widely used to estimate the oxidative potential (OP) of PM. Several epidemiological studies employing DTT assays have shown that the oxidative stress induced by PM is primarily attributed to the presence of reactive chemical constituents, encompassing both inorganic and organic compounds, as well as trace metals (Charrier and Anastasio, 2012; Fang et al., 2016; Gao et al., 2020; Verma et al., 2015a). Particularly, OP was found to be sensitive to the amount of organic matters and heavy metals, and well correlated with elemental carbon (EC), organic carbon (OC), water-soluble organic

* Corresponding author.
E-mail address: meehye@korea.ac.kr (M. Lee).
[1] These authors contributed equally to this work.

https://doi.org/10.1016/j.envint.2025.109424
Received 8 January 2025; Received in revised form 23 March 2025; Accepted 27 March 2025
Available online 9 April 2025

carbon (WSOC), and Ni, Zn, As, V, Cd, and Pb (e.g., Bae et al., 2017; Lovett et al., 2018). In addition, water-soluble total carbon (WSTC) and atmospheric humic-like substances (HULISs), such as quinone, hydroquinone, and oxygen-rich organics, have been reported to be a main factor determining the OP of PM (e.g., Ayres et al., 2008; Bates et al., 2015; Charrier and Anastasio, 2012; Verma et al., 2015b; Xiong et al., 2017). However, considering the complexity of aerosol composition, a comprehensive interpretation of bulk aerosol properties is more significant than isolating and evaluating the contributions of individual components to DTT oxidative activities (Chen et al., 2019).

PM is a complex mixture of chemical compounds that are formed in or emitted into the atmosphere from various sources, such as industrial processes, fuel utilization, biomass burning, and human activities. Recent shifts in energy policy toward the adoption of clean energy, have impacted the mass and compositions of PM and, consequently, potential health effects (Ding et al., 2019; Lang et al., 2017; Park et al., 2018; Zhang et al., 2019; Joo et al., 2024).

Seoul, the capital of South Korea, has a population of approximately ten million and, the broader Seoul Metropolitan Area-including its surrounding satellite cities-hosts more than half of the nation's population. Geographically, Seoul is situated in a mountainous and hilly region, with elevated terrain along its northern boundary and the Han River flowing through its center. As of recent statistics, over three million vehicles are registered in the city. Emissions from these vehicles comprise a complex mixture of organic and inorganic pollutants, including nitrogen oxides (NOx), volatile organic compounds (VOCs), and heavy metals. These emissions are major precursors to the formation of ozone (O_3) and fine particulate matter smaller than 2.5 μm in diameter ($PM_{2.5}$), which pose significant environmental and public health concerns. In a recent study, the findings of Korea-United States Air Quality (KORUS-AQ) underscored that, despite significant emissions in the Seoul Metropolitan Areas (SMA), the air quality intricately influenced by synoptic meteorological conditions (Kim et al., 2020a; Miyazaki et al., 2019; Peterson et al., 2019). Under the strong influence of the monsoon system, Northeast Asia exhibits distinct seasonal variations in the concentrations of atmospheric trace constituents, primarily reflecting the origin of air masses. During summer, air masses are predominantly transported from the southeastern ocean, while in winter, they originate mainly from the northwestern Asian continent. This seasonal shift is a defining meteorological feature of the Korean Peninsula including Seoul (Kim et al., 2020b; Savic et al., 2024).These results highlight the necessity of delving into not only the composition of $PM_{2.5}$ but also its formation processes and emission sources to accurately assess the OP of urban $PM_{2.5}$ in northeast Asia.

The primary objective of this study is to assess the oxidative potential (OP) of urban $PM_{2.5}$ using the DTT assay and to identify the key factors influencing $PM_{2.5}$ OP. A total of 75 $PM_{2.5}$ samples were collected from an urban site in Seoul between 2019 and 2021. In addition to OP measurements via the DTT assay, comprehensive chemical characterization was performed, including the determination of water-soluble ions, carbonaceous components, and trace metal elements. To further elucidate the emission sources contributing $PM_{2.5}$, carbon and nitrogen isotopic analyses ($\Delta^{14}C$, $\delta^{13}C$, and $\delta^{15}N$) were conducted to provide source-specific signatures. The findings of this study are expected to provide valuable insights for developing effective strategies to mitigate urban air pollution.

2. Materials and methods

2.1. $PM_{2.5}$ sample collection

The experiment was conducted at the Korea University campus located in the northeastern part of Seoul (37.59° N, 127.02° E; Fig. 1). $PM_{2.5}$ samples were collected on quartz filters (20 × 25 cm; Pallflex Products, USA) using a high-volume sampler (3000 series, Ecotech, Australia) installed on the rooftop of Hana Science Hall in 2019 ~ 2021 and Mediheal Earth and Environmental Science Hall in 2021. Quartz filters were pre-baked at 550 °C to remove organic impurities. Sampling duration varied from 1 to 3 days, depending on meteorological conditions, to ensure sufficient particle mass for analysis and to differentiate

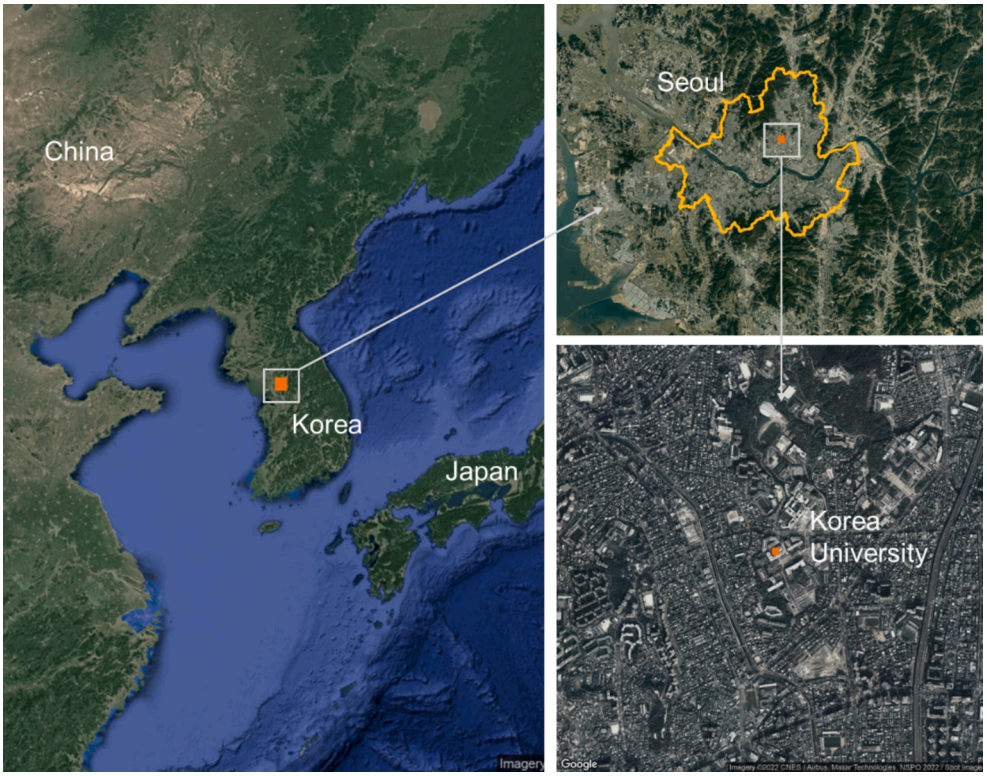

Fig. 1. Study areas and location of the $PM_{2.5}$ sample collection.

airmass characteristics. At least one sample was collected per month, excluding the summer months from July to September (Table 1).

Meteorological suites including temperature, relative humidity, and wind direction and speed were measured on campus. Additionally, hourly data on criteria air pollutants–including $PM_{2.5}$ and PM_{10} mass concentrations, as well as mixing ratios of O_3, NO_2, CO and SO_2– were obtained from a nearby air quality monitoring station located approximately 1 km to the south and utilized for further analysis (https://www.airkorea.or.kr/).

2.2. Oxidative potential assessment using DTT assay

The oxidation potential (OP) of $PM_{2.5}$ samples were evaluated using the following procedure. Filters were punched in sizes of 2 cm^2 and 5 cm^2 for the warm season (April–October) and cold season (November–March), respectively. The punched filters were soaked in 10 mL of deionized water (18.2 MΩ, Millipore, Bedford, MA, USA) and sonicated three times for 30 min each. The extract was filtered through a 0.45 μm syringe filter to remove insoluble components.

The OP of the water-soluble extracts was evaluated using the DTT assay, following the protocol suggested by Wang et al. (2019). Briefly, 1.75 mL of $PM_{2.5}$ extracts and 4.55 mL of 0.1 M potassium phosphate (pH 7.4) were dispensed into a 10-mL glass vial and the mixture was incubated at 37 ℃ oven for 5 min; 0.7 mL of 1 mM DTT was added and 0.5 mL aliquot was transferred to another tube preloaded with 0.5 mL Trichloroacetic Acid (TCA,10 % w/v) after incubation for 0, 10, 20, and 30 min. 2 mL of Tris-base which is 0.4 M Tris with 20 mM EDTA (pH 8.9) mixed with 50 μL of 10 mM 5,5′-dithiobis-2-nitrobenzoic acid (DTNB) was added, leading to a reaction between DTT and DTNB to form 2-nitro-5-benzoic acid (TNB). After 5 min of incubation at room temperature, residual DTT was quantified immediately by measuring the absorbance spectrum using a UV–visible spectrometer at 412 nm. The final DTT consumption of each extracted $PM_{2.5}$ sample was corrected with a blank and then normalized by the total volume (DTTv) and mass (DTTm) of air sampled using the following Eqs. (1)–(2):

$$\mathrm{DTTv}\left(\mathrm{nmol}\,min^{-1}\,m^{-3}\right) = \frac{r_s\left(nmolmin^{-1}\right) - r_b\left(nmolmin^{-1}\right)}{V_t(m^3) \times \frac{A_h(cm^2)}{A_t(cm^2)} \times \frac{V_s(mL)}{V_e(mL)}} \quad (1)$$

$$\mathrm{DTTm}\left(\mathrm{nmol}\,min^{-1}\,g^{-1}\right) = \frac{r_s\left(nmolmin^{-1}\right) - r_b\left(nmolmin^{-1}\right)}{M_t(g) \times \frac{A_h(cm^2)}{A_t(cm^2)} \times \frac{V_s(mL)}{V_e(mL)}} \quad (2)$$

where, r_s and r_b are the DTT consumption rates of the sample and the blank, respectively. V_t and V_t are the total sampling volume (m^3) and $PM_{2.5}$ mass (g), respectively. A_h and A_t are the areas of the hole and total filter, respectively. V_s and V_e are the sample volumes participating in the reaction and extraction volume, respectively.

Multiple control tests, including blank (n = 24, deionized water), field blank (n = 6, ambient quartz filter), and positive control (n = 24, 9,10-phenanthrenequinone), were performed to verify the reproducibility of the DTT assay. The average rate had a coefficient of variation (CV %) of 10.8, 13.8, and 1.10 % in each control group, which were within the acceptable limits. The results of the precision of the DTT assay using blank and positive controls are presented in Table 2. Pearson's correlation between DTTv and chemical components was calculated using MATLAB, and significance was considered at $p < 0.05$.

Table 1
Monthly sample number of $PM_{2.5}$ collected during 2019–2021 in this study.

	2019	2020	2021
Jan	2	1	1
Feb	–	4	–
Mar	–	12	4
Apr	–	8	
May	9	12	
Jun	–	11	
Oct	1	1	–
Nov	–	7	–
Dec	2	–	–
Total	14	56	5

2.3. Chemical analysis of $PM_{2.5}$

The main constituents of $PM_{2.5}$ were analyzed, including water-soluble ions, WSOC, water-soluble total nitrogen (WSTN), OC, EC, and metal concentrations. For analysis, quartz filters were punched to 1 cm × 1.5 cm, two of which were extracted in 20 mL 18 MΩ Milli-Q water via sonication for 30 min. The liquid extract was then filtered using a 0.22 μm PTFE disposable syringe filter. Eight water-soluble ions, including SO_4^{2-}, NO_3^-, Cl^-, NH_4^+, K^+, Na^+, Ca^{2+}, and Mg^{2+}, were determined using an ion chromatography (Methrohm Eco IC, Switzerland). More details about the analysis method can be found in Lim et al. (2022).

WSOC and WSTN of $PM_{2.5}$ were analyzed using a total organic carbon (TOC)/total nitrogen (TN) analyzer (TOC-L, TNM-L, Shimadzu, KBSI Meteropolitan Seoul Center). In order to determine the WSOC, non-purgeable organic carbon (NPOC) method was applied, which involves injecting acid to lower the pH to 3 or less, sparging purified air to remove inorganic carbon and volatile organic carbon, followed by combustion catalytic oxidation at 680 °C to provide CO_2. The detection limit was 0.04 mg/L or less. WSTN was analyzed using a catalytic combustion method with chemiluminescence at 720 °C, with a detection limit of 0.05 mg/L. WSON was calculated using the water-soluble inorganic nitrogen (NO_3-N, NH_4-N), which was subtracted from the WSTN. EC and OC of $PM_{2.5}$ were analyzed using an OC-EC analyzer (Sunset Laboratory Inc., Portland, OR) with the thermo-optical transmittance method and NIOSH8710 protocol at Ewha Woman's University. The same extracts were used for the analysis of water-soluble metal components and quantitative analysis was performed using ICP-MS (7700 Series, Agilent Technologies, Inc., USA).

2.4. Isotope analysis

Out of 75 $PM_{2.5}$ filter samples, isotopic compositions, including $\Delta^{14}C$, $\delta^{13}C$, and $\delta^{15}N$, were analyzed for 60 samples at the University of California, Irvine (UCI). The stable carbon and nitrogen isotopic ratios of TC and TN ($\delta^{13}C$ and $\delta^{15}N$) were analyzed with an elemental analyzer (EA, Fisons NA-1500NC, Thermo, Waltham, MA, USA) coupled to an isotope-ratio mass spectrometer (IRMS, DeltaPlus XL, Thermo) (Xu et al., 2007). For this analysis, the one or pieces of filter were cut out with a punch (SP-15, 1 cm × 1.5 cm, Sunset Laboratory, Portland, OR, USA) and weighed in tin capsules (5 mm × 9 mm, 041,077, Costech Analytical Technologies, Valencia, CA, USA). Stable isotope ratios, δ (‰) is defined as $(R_{sample}/R_{standard} - 1) \times 1000$, where R is the ratio of $^{13}C/^{12}C$ for stable carbon isotope and $^{15}N/^{14}N$ for stable nitrogen isotope and R_{sample} ($R_{standard}$) is the R of a sample (the international standard). Standards and field blanks were analyzed along with samples, and their $\delta^{13}C$ values are reported relative to Vienna Pee Dee Belemnite (VPDB) and air for $\delta^{15}N$ with correction for filter and field blanks; uncertainty was 0.1 ‰ for $\delta^{13}C$ and 0.2 ‰ for $\delta^{15}N$ (1σ from long-term measurements of secondary standards). International Atomic Energy Agency and U.S. Geological Survey ammonium sulfate standards IAEA-N-1, IAEA-N-2, USGS25, and USGS26.

For the radioactive carbon isotopic ratios of TC ($\Delta^{14}C$), several pieces

Table 2
Precision performance of DTT assay for blank and positive controls.

Samples	Number	Average rate (nmol/min)	SD	%CV[a]
Deionized water	24	0.591	0.064	10.8
Field blank	6	0.491	0.068	13.8
Positive control	24	4.931	0.054	1.10

[a] Coefficient of variation (% CV) = SD / Average · 100.

of filter were sealed with CuO under vacuum and combusted at 900 °C for 3 h, yielding the CO_2. The CO_2 of sample or blank was cryogenically purified and reduced to graphite using a sealed-tube zinc-reaction technique (Xu et al., 2007). The graphite was then analyzed together with graphitization standards and blanks by accelerator mass spectrometry (AMS; NEC 0.5 MV 1.5SDH-1, National Electrostatics Corporation, Middleton, WI). The $\Delta^{14}C$ values are first calculated from ^{14}C and reported as f_M with ^{13}C fractionation correction, using online AMS $^{13}C/^{12}C$ calculations. The uncertainty was 2 ‰–3‰ (1 SD for long-term secondary standard analyses) for modern samples.

$$f_m = \frac{\frac{^{14}C}{^{12}C}(sample)}{\frac{^{14}C}{^{12}C}(sample)} = \frac{F^{14}C_{modern}}{F^{14}C_{modern}}$$

2.5. Cluster analysis of backward trajectories

Using the Hybrid Single Particle Lagrangian Integrated Trajectory (HYSPLIT) model version 4 (Draxler et al., 2016), air mass trajectories arriving in Seoul (37.59 N, 127.03 E) at 500 m were calculated every hour backward for 2 days (48 h), from January 2019 to December 2021. Global Data Assimilation System (GDAS; 1 × 1) data were used as the input for the HYSPLIT model. With these backward trajectories, cluster analysis was conducted using the openair library in R.

3. Results and discussion

3.1. Characterization of the chemical composition and oxidative potential of $PM_{2.5}$

For the entire experiment period, the mean (±SD) value of OP was 0.58 ± 0.48 nmol m^{-3} min^{-1} and the average mass concentration of $PM_{2.5}$ was 29.2 ± 13.0 μg m^{-3}. It is noteworthy that when $PM_{2.5}$ reached the maximum (55.0 μg m^{-3}), DTTv showed the highest value of 2.01 nmol m^{-3} min^{-1}. In comparison, the urban area of Hong Kong and Hangzhou exhibited similar $PM_{2.5}$ mass (24.1 μg m^{-3} and 20.7 μg m^{-3}, respectively) and DTTv value (0.58 nmol m^{-3} min^{-1} and 0.62 nmol m^{-3} min^{-1}, respectively) to those of this study (Li et al., 2021, Cheng et al., 2021). In general, DTTv value was reported to be high in high $PM_{2.5}$ conditions, indicating an overall dependence of DTTv on PM mass: DTTv was 1.16 nmol m^{-3} min^{-1} with $PM_{2.5}$ of 91.4 μg m^{-3} in Changzhou during spring (Wang et al., 2019) and an annual average of DTTv was 12.26 ± 6.82 nmol m^{-3} min^{-1} with 113.8 ± 62.7 μg m^{-3} of $PM_{2.5}$ in Beijing during 2015 ~ 2016 (Yu et al., 2019). In Beijing, however, the seasonal mean of DTTv was highest during summer when $PM_{2.5}$ was the lowest. Therefore, it is also suggested that DTT values cannot be solely attributed to $PM_{2.5}$ mass concentrations.

Considering the distinct seasonality in East Asia, measurements were divided into two groups: the warm season from April to October and cold season November to March. The mean ± standard deviation of DTTv was 0.65 ± 0.55 nmol m^{-3} during the cold season and 0.48 ± 0.37 nmol m^{-3} during the warm season. This seasonal difference can be primarily related to $PM_{2.5}$ mass, of which mean was 34.4 ± 12.7 μg m^{-3} and 25.0 ± 10.0 μg m^{-3} in the cold and warm season, respectively (Table 2). Accordingly, a substantial contrast was observed in both the mass concentration and the relative abundance of major constituents during the two periods (Fig. 2). While NO_3^- dominated under high $PM_{2.5}$ conditions in the cold season, SO_4^{2-} and OC concentrations remained almost constant during two seasons. As a result, the relative abundance of major constituents showed a sharp contrast between the two seasons. The contribution of SO_4^{2-} and OC to $PM_{2.5}$ mass was substantially elevated in the warm season under low $PM_{2.5}$ conditions. The production of particulate nitrate is generally favorable in cold seasons when precursor emissions are elevated. In contrast, the oxidation of SO_2 and organic compounds is typically faster during summer than winter (Kim et al., 2020b). Among inorganic ions, generally derived from soil minerals or sea salt, the contribution of Na^+, Cl^-, and K^+ to $PM_{2.5}$ mass was more

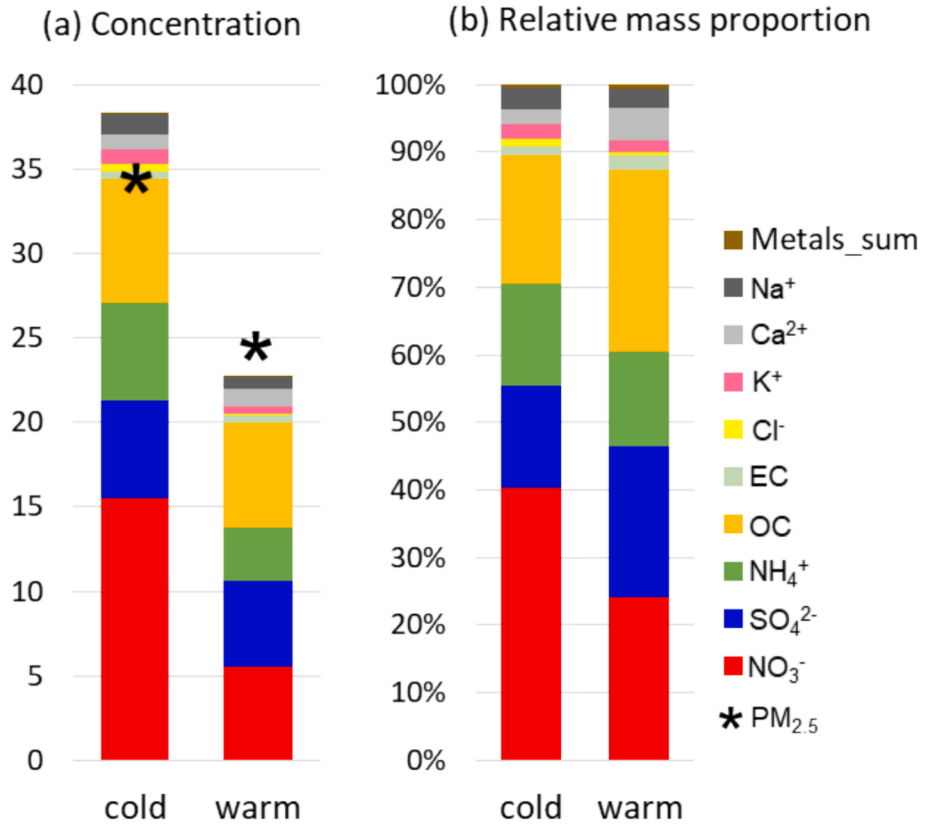

Fig. 2. Concentrations and relative proportions of major $PM_{2.5}$ components in warm and cold seasons.

significant in the cold season than in the warm season. The opposite tendency was observed for Mg^{2+} and Ca^{2+}. Similarly, the warm season exhibited a greater relative abundance of soluble metal species compared to the cold season, although they accounted for only 0.4 % of the total $PM_{2.5}$ in this study.

3.2. Determining factors of $PM_{2.5}$ oxidative potential

The relationship between the oxidative potential and chemical composition of $PM_{2.5}$ was examined to identify key factors that play a crucial role in causing oxidative stress. We first analyzed the Pearson correlation coefficient (r) between the chemical composition and DTTv for all samples and then compared those between the two seasons (Table 3). While the overall correlation coefficient between DTTv and $PM_{2.5}$ was 0.39, it was significantly higher during the cold season compared to the warm season. In particular, DTTv showed a moderately strong correlation with secondary inorganic ions during the cold season and with EC during the warm season. Similarly, a previous study conducted in China (Wang et al., 2019) also reported a pronounced diurnal and seasonal variations at an average $PM_{2.5}$ concentration of 63 μgm^{-3}. Given that correlation coefficient (|r|) exceeding 0.3 suggests moderately strong correlations, and considering that the average $PM_{2.5}$ concentration in this study (29.1 μgm^{-3}) was less than half of that reported by Wang et al. (2019), our analysis revealed significant correlations between $PM_{2.5}$ mass, its major constituents, and DTTv. Interestingly, transition metals were found to contribute little to the oxidative potential of $PM_{2.5}$ in this study.

DTTv was relatively correlated well with secondary inorganic ions and carbonaceous compounds, including NO_3^-, NH_4^+, Cl^-, OC, EC, and TC (r = 0.4) over the entire period. The correlation coefficients of these species with DTTv were notably strengthened (r > 0.5) during the cold season, coinciding with elevated $PM_{2.5}$ mass concentrations (Fig. 2). In particular, the r values for NO_3^- and NH_4^+ were 0.58 and 0.56, respectively. Particulate nitrates stand out as a prominent contributor to severe haze pollution in East Asian urban areas during the cold season (Kim et al., 2020a, Jo et al., 2022; Kang et al., 2022; Kim et al., 2022) Although the relative abundance of SO_4^{2-} and OC were higher in the warm season than in the cold season, the correlation of those species with DTTv were better in the cold season than in the warm season. Overall, our results demonstrate the dependence of DTTv on the mass concentrations of the primary components of $PM_{2.5}$.

TC (the sum of OC and EC) and OC demonstrated significantly stronger correlations with DTTv than WSOC. Organic compounds, such as PAHs and quinone, are known to directly contribute the reduction of DTT concentration. Previous studies have also reported that a strong correlation between DTTv and NO_3^-, NH_4^+, and SO_4^{2-}, indicating that DTTv effectively reflects the overall mass levels of $PM_{2.5}$, as redox-active oxidized organic compounds often co-vary with inorganic ions (Gao et al., 2020; Li et al., 2018; Verma et al., 2009; Win et al., 2018; Yu et al., 2022). The relatively strong correlations observed in this study between TC, NH_4, NO_3 and DTTv suggests this covariation and emphasize the practical importance of nitrogen and carbon emission sources.

During the cold season, K^+ (r = 0.39) and Cl^- (r = 0.56) showed reasonably strong correlations with DTTv, suggesting a connection between emission sources and oxidative potential. This is consistent with their roles as markers for biomass or coal combustion emissions (Cheng et al.,2013; Liang et al.,2021; Pachon et al., 2013; Srivastava et al., 2021; Wang et al., 2022; Yu et al., 2018). In contrast, during the warm season, there was virtually no correlation between DTTv and $PM_{2.5}$ mass or its major components, except for EC (r = 0.34). Since EC, equivalent to BC, is primarily emitted by automobiles in Seoul (Lim et al., 2023), this finding highlights the influence of vehicle emissions.

Transition metals such as Fe, Cu, and Mn are known to be redox-active, with Fe (Fe^{2+} and Fe^{3+}) catalyzing OH radical formation and Cu and Mn exhibiting high DTT activity in biological systems (Charrier and Anastasio, 2011, Kajino et al., 2021; Lin and Yu, 2011, Lovett et al., 2018; Xiong et al., 2017; Yu et al., 2022). However, the relationships with DDT activity and metals often depend on their associations with organic compounds. In this study, DTTv showed weak or even negative correlation with transition metals, including Fe and As, particularly during the warm season. Similarly, a study conducted in Atlanta, USA, reported that the predictive power of transition metals for oxidative stress varied by season and that these elements were not reliable indicators of oxidative stress, likely due to their redox-inactive properties. These results suggest that the contribution of transition metals to $PM_{2.5}$ toxicity may be limited under conditions of low PM mass concentrations, highlighting the need for further investigation into the specific roles of metal constituents in aerosol-induced oxidative stress (Liu et al., 2023).

Given the overall tendency of OP depending on the mass and the season, the relationship between DTTv and mass concentrations of each $PM_{2.5}$ components were investigated: The entire range of DTTv was divided into quartiles (0.2, 0.5, and 0.8 for the 25th, 50th, and 75th percentile), for which the concentrations of all measured species were compared (Fig. 3). The highest quartiles of DTTv (>0.8) were associated with higher $PM_{2.5}$ mass concentrations and correspondingly higher concentrations of secondary inorganic ions including NO_3^-, SO_4^{2-}, and NH_4^+. It is noteworthy that Cl^- concentration almost linearly increased with DTTv. As mentioned above, Cl^- is mainly generated during combustion processes, such as those associated with coal or biomass (Dai et al., 2020; Srivastava et al., 2021; Wang et al., 2023). Given that high $PM_{2.5}$ mass events typically coincide with the elevated levels of CO and NO_2 during the cold season, these results suggest a significant impact from combustion sources in winter (Gil et al., 2023; Lee et al., 2022). On the contrary, in the lowest quartile range of DTTv (< 0.2), the majority of constituents exhibited consistently low concentrations under low wind speed, reflecting the characteristics of warm season. The highest concentrations of total soluble metals and water-soluble organic nitrogen (WSON) corresponding to the highest DTTv values align with the

Table 3
Pearson correlation between DTT_v and chemical components of $PM_{2.5}$. Values are correlation coefficient (r). Values in bold letters show moderately correlation (|r| > 0.3), and * denote significant correlations (α = 0.05).

r	DTT_v		
	Overall	Cold	Warm
PM2.5	**0.39**	**0.50**	0.17
PM10	**0.30**	**0.32**	0.23
OC	**0.40**	**0.51**	0.26
EC	**0.36**	**0.42**	**0.34**
TC	**0.40**	**0.51**	0.26
WSON	−0.07	−0.13	−0.14
WSOC	0.13	0.07	0.09
NH_4^+	**0.40**	**0.58**	0.08
NO_3^-	**0.40**	**0.56**	0.08
SO_4^{2-}	0.27	**0.48**	0.03
Na^+	0.08	0.04	0.0
K^+	**0.33**	**0.39**	0.11
Ca^{2+}	0.11	0.12	0.16
Mg^{2+}	0.11	0.03	0.19
Cl^-	**0.40**	**0.56**	0.17
Li	−0.16	−0.17	**−0.30**
Al	0.01	0.26	**−0.30**
Sc	−0.10	−0.24	0.05
Ti	0.06	**0.37**	−0.25
V	0.00	0.10	0.02
Cr	−0.12	−0.20	−0.16
Mn	−0.14	−0.04	−0.27
Fe	−0.18	−0.02	**−0.38**
Co	−0.11	−0.14	−0.21
Ni	−0.14	−0.20	−0.22
Cu	−0.09	0.04	−0.22
Zn	−0.10	−0.12	−0.15
As	−0.22	−0.06	**−0.37**
Y	−0.0	0.30	−0.24
Cd	−0.07	0.00	−0.19
Pb	−0.03	0.14	−0.19

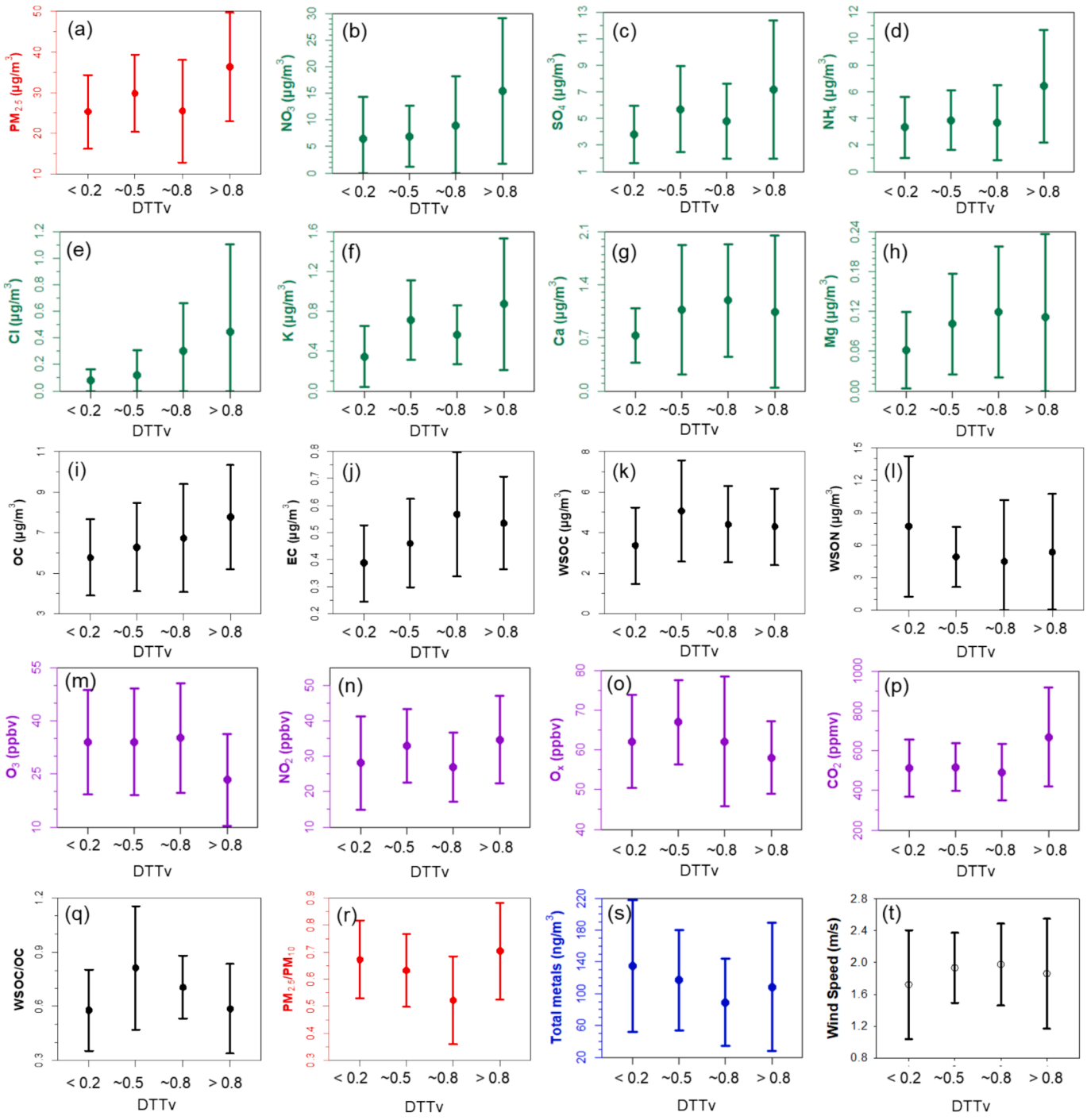

Fig. 3. Distributions of the $PM_{2.5}$ mass and mean concentrations and standard deviation (σ) of major components, as well as the concentrations of gaseous O_3, NO_2, and CO, amd $PM_{2.5}/PM_{10}$ ratio as the certain DTTv range (nmol m^{-3} min^{-1}).

substantial correlation between EC and DTTv observed during the warm season (Table 2), emphasizing the predominant impact of vehicle emissions under stagnant conditions.

Additionally, the $PM_{2.5}/PM_{10}$ ratio showed a minimum value in the third quartile range of DTTv (0.5 ~ 0.8), mirroring the trend observed for Ca^{2+} and Mg^{2+}. This highlights the impact of soil minerals contributing significantly to the increase in PM_{10} during Asian dust events. The second DTTv quartile is characterized by the highest WSOC and Ox (O_3 + NO_2) concentration, and WSOC/OC ratio, demonstrating that oxidative potential is related to atmospheric oxidation processes. Interestingly, K^+ and $PM_{2.5}$ exhibited a similar response to DTTv. These results are consistent with those reported in previous studies that pointed out biomass burning as a key contributor to oxidative potential (Cheng et al., 2013; Liang et al., 2021; Pachon et al. (2013); Yu et al., 2018; Glojek et al., 2024).

These findings underscore the significance of a detailed analysis of the correlation between DTTv and specific constituents, such as organic matter or inorganic ions, for gaining insights into the oxidative potential of $PM_{2.5}$ in urban Seoul. Additionally, the results reveal that the oxidative potential represents a complex interplay of various chemical components. The dynamics of this relationship may vary depending on local and transported sources (e.g., vehicle emissions, biomass burning, and mineral dust), as well as atmospheric processing (e.g., oxidation) and synoptic meteorological conditions. Hence, the influence of

synoptic meteorology and source signatures are examined in detail in the following sections.

3.3. Air mass history and oxidative potential

A cluster analysis was conducted on air mass trajectories spanning the year 2019 to 2021. The 48-hour backward trajectories of air mass reaching Seoul at 500 m altitude were categorized into six distinct groups (Fig. 4a). Clusters C1 and C2, represent trajectories of air masses moving from the northwest through lower and higher altitudes, respectively, and account for 34 % of the total. Air masses from eastern China, the East China Sea, and the East Sea classified as C3 (14 %), C5 (11.4 %), and C6 (14.7 %) clusters, respectively. As the shortest trajectory, C4 (25.5 %) represents stagnant condition of the atmosphere. In the study region, these clusters are intricately linked to atmospheric circulation patterns and seasonal variations. When compared to the concentration-weighted trajectories of $PM_{2.5}$ that was analyzed in R (Hsu et al., 2003) (Fig. 4b), $PM_{2.5}$ concentrations exhibit a clear elevation in the outflows from eastern China, particularly in the region extending from Hebei to Nanjing.

In line with the relationship between DTTv and chemical components illustrated in Fig. 3, the relative abundance of the six clusters were compared against the interquartile range of DTTv (Fig. 5). When DTTv was below the median value of 0.5, C4 and C5 cluster were the most frequent. In contrast, trajectories from continent, including C1, C2, and C3 were predominant at higher DTTv levels that exceeded the median. Due to the Asian monsoon, C1 and C2 are typically observed during winter, while C5 and C6 are more prevalent in summer. The relative abundance of C1 increased with higher DTTv levels. As reported by Ham et al (2021), air influenced by outflows from northeastern China (C1) exhibited significantly elevated levels of organic carbon (OC) attributed to combustion activities related to heating. In comparison, the relative abundance of C2 was notably high in the third quartile range of DTTv, suggesting the influence of soil minerals. This observation is consistent with elevated concentrations of Ca^{2+} and Mg^{2+}, as well as the lowest ratios of $PM_{2.5}/PM_{10}$ (Fig. 3).

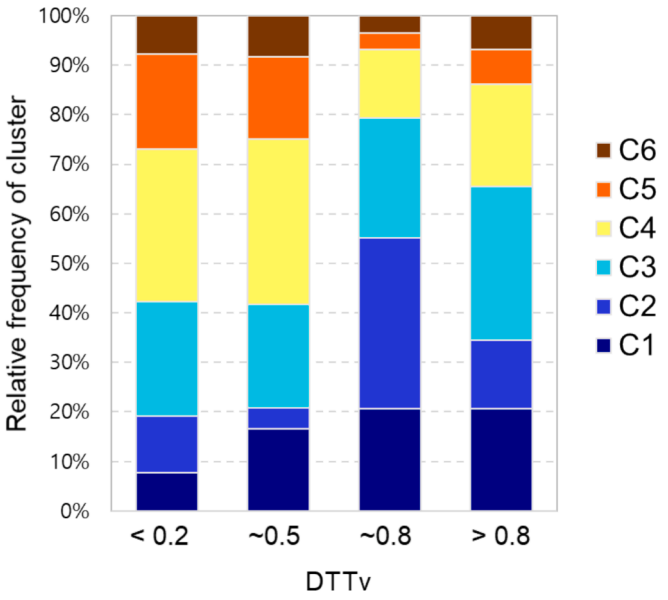

Fig. 5. Relative frequency of air mass backward trajectories according to DTTv level (nmol m^{-3} min^{-1}).

It is noteworthy that C3 cluster that was the most frequent at the highest DTTv, passed through areas with elevated $PM_{2.5}$ concentrations, as shown in Fig. 4b. This finding is in good agreement with the results from previous studies that identified it as a major source region for $PM_{2.5}$ and NO_3^- (Kim et al., 2020b). In this study, the correlation between DTTv and NO_3^-concentration was the most pronounced (Fig. 3).

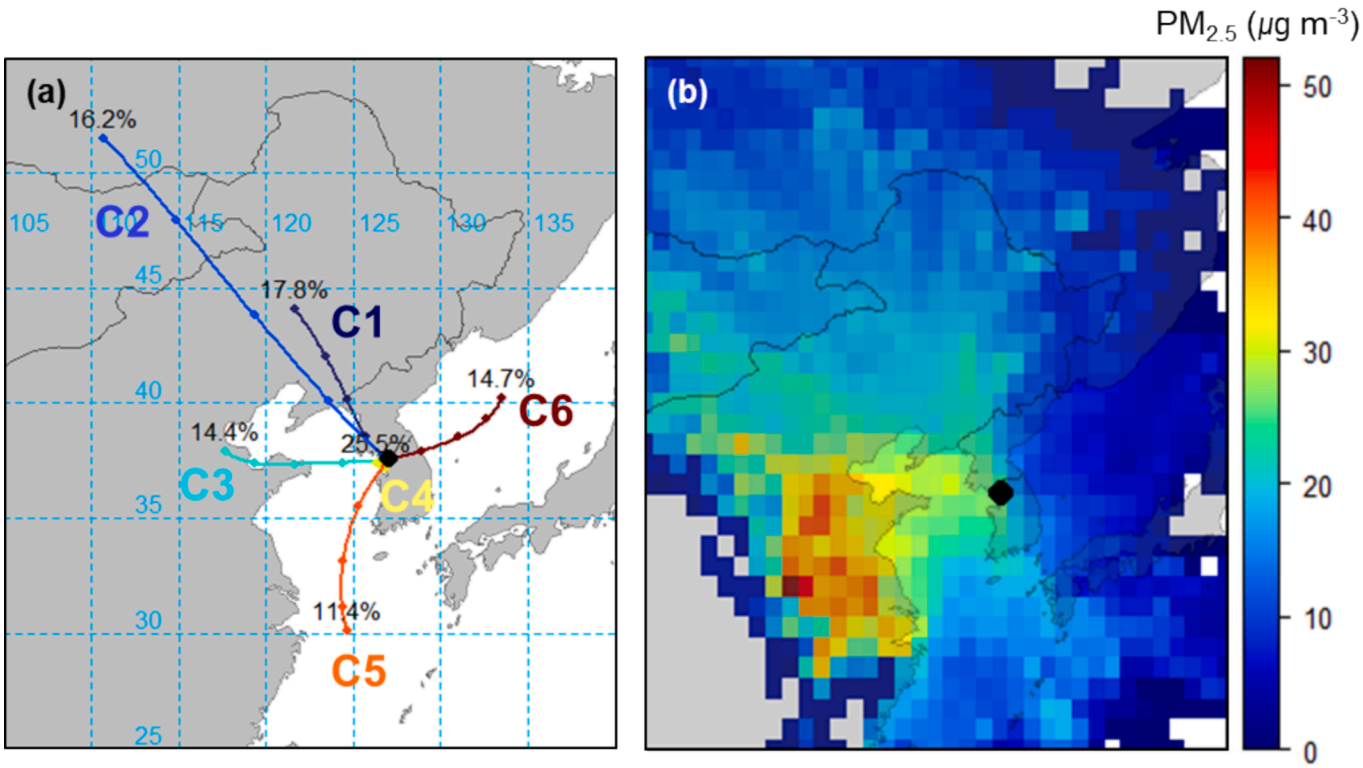

Fig. 4. Six trajectories classified from air mass clusters using NOAA HYSPLIT-4 model at 500 m for 48-h backward trajectories (a), and concentration weighted trajectories (CWT) for $PM_{2.5}$ (b) from 2019 to 2021.

3.4. Isotope (14C, $\delta^{13}C$ and $\delta^{15}N$) source signatures and DTT activities

To estimate emission sources of $PM_{2.5}$ with high oxidative potential, the isotopic composition of the total carbon (TC) and total nitrogen (TN) were analyzed. In this study, f_m represents the fraction of non-fossil sources contributing to the total carbon, expressed as a value between 0 and 1. Across all measurements, f_m ranged from 0.43 to 0.76, with a mean of 0.62, consistent with previous observations in Seoul (Lim et al., 2022). While the mean f_m was similar in both seasons, its variability was greater in summer than in winter across all four DTTv levels (Fig. 6a). Notably, at low DTTv levels, f_m was significantly lower in summer than in winter. This finding suggests that the oxidative potential of $PM_{2.5}$. is more strongly linked with fossil fuel sources during the warm season, particularly when $PM_{2.5}$ levels are low.

The carbon stable isotope ratio, $\delta^{13}C$, proves valuable in discerning the type of fuel combustion from which the precursors of a carbonaceous aerosol originated. The $\delta^{13}C$ fingerprints vary in a narrow but distinctive range: –25.5 ± 1.3 ‰ for liquid fossil (Chen et al., 2012; Gleason et al., 1984; Lim et al., 2022b; Tang, 2001; Widory, 2006), –23.4 ± 1.3 ‰ for solid fossil (Agnihotri et al., 2011; Ancelet et al., 2011; Chen et al., 2012; Kawashima et al., 2012; Tanner et al., 1989; Widory, 2006), and –26.7 ± 1.8 ‰ for C3 plant (Agnihotri et al., 2011; Bird and Ascough, 2012; Chen et al., 2012; Kawashima et al., 2012), representing emissions from vehicle exhaust, coal combustion, and biomass combustion such as paddy, respectively (Lim et al., 2022).

The relationship between $\delta^{13}C$ and the quartile range of DTTv is shown in Fig. 6b. During the cold season, $\delta^{13}C$ was most depleted in the first DTT quartile and enriched in the upper quartile. These results suggest that low levels of DTTv were strongly influenced by liquid fossil fuels, whereas higher DTTv levels correspond to an increasing contribution of solid fossil fuels to $PM_{2.5}$ mass. As presented in Fig. 6d, $PM_{2.5}$ concentrations were highest in the upper quartile of DTTv, predominantly observed in winter samples, where $\delta^{13}C$ values were slightly decreases. It is noteworthy that the highest quartile of DTTv was associated with the air mass clusters originating from eastern China (C3), where $PM_{2.5}$ concentrations were the highest and being stagnated (C4) (Fig. 5). The shortest trajectories of these air masses indicate that aged particles likely played a significant role in increasing oxidative stress (Liu et al., 2023). Additionally, elevated Cl^- and K^+ concentrations in the same quartile father highlight the impact of biomass burning (Fig. 3).

During the warm season, $\delta^{13}C$ values were generally lower than in the cold season, reflecting a reduced influence of solid fossil fuel combustion and an increased contribution from liquid fossil fuels under stagnated air conditions. The lowest $\delta^{13}C$ in the highest DTT interval is consistent with the $\Delta^{14}C$ signature, indicting a higher contribution from non-fossil sources.

The $\delta^{15}N$ values exhibited a decreasing trend with increasing DTTv during the warm season (Fig. 6c). Higher $\delta^{15}N$ values are attributed to the strong fractionation effect between NH_3 and NH_4^+ at elevated temperatures. Previous studies have demonstrated that in Seoul, the $\delta^{15}N$ of the total nitrogen (TN) in $PM_{2.5}$ was primarily determined by $\delta^{15}N$ of ammonium (NH_4), which is predominantly derived from fossil fuel sources (Lim et al., 2020; Lim et al., 2022). In contrast, the winter $\delta^{15}N$ values were at their lowest in the first quartile of DTTv, corresponding to low $PM_{2.5}$ levels. These samples were associated with to air masses originating mostly from the northeaster China in winter, indicating an increased contribution from non-fossil sources like livestock waste (Lim et al., 2022).

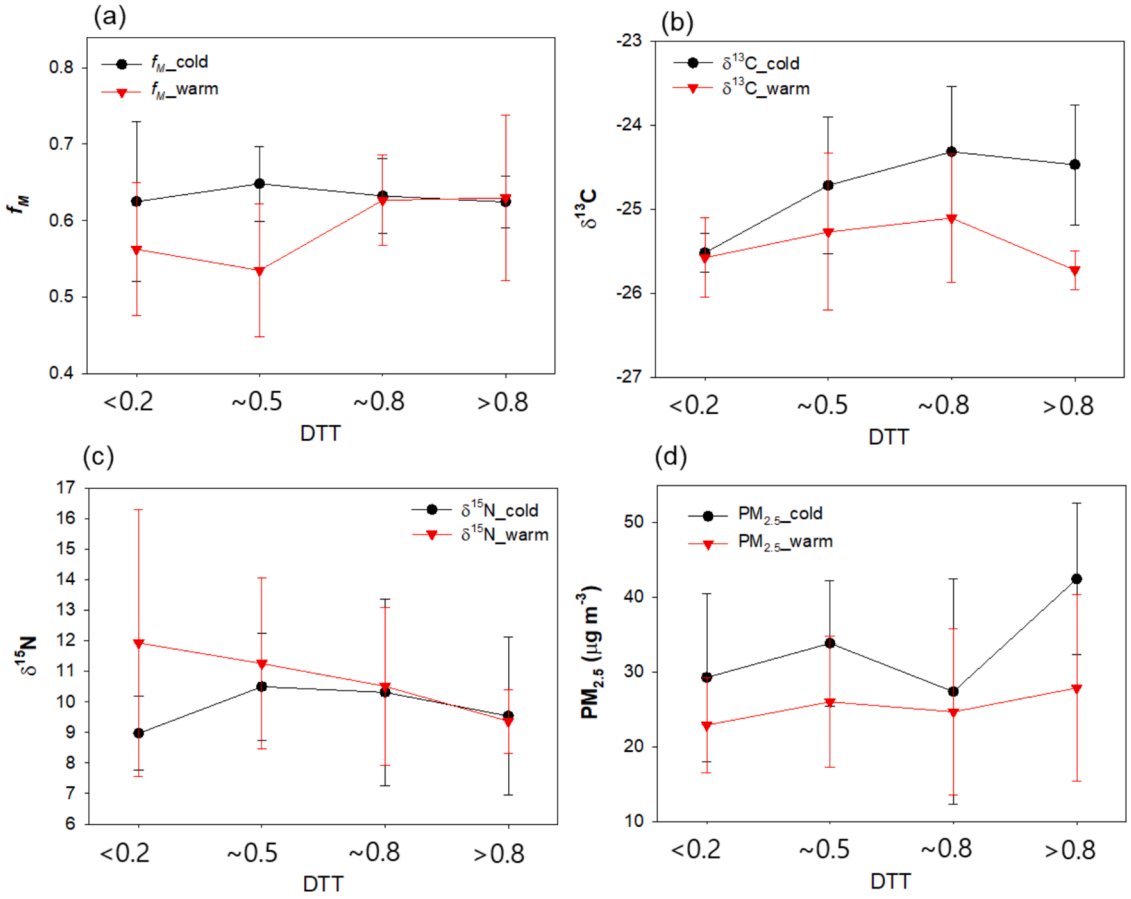

Fig. 6. Average isotope values (f_M, $\delta^{13}C$ and $\delta^{15}N$) and $PM_{2.5}$ mass concentrations for cold and warm seasons by DTTv level. Black circles indicate cold season, red inverted triangles indicate warm season. Error bars represent the mean standard deviation (1 σ). (For interpretation of the references to colour in this figure legend, the reader is referred to the web version of this article.)

Apart from the sharp contrast in $\delta^{15}N$ observed at the lowest quartile of DTTv, $\delta^{15}N$ values across both seasons indicate a consistent signature from vehicle emissions, likely due to the co-emission of nitrogen and carbon precursors. These findings highlight the need for future research to refine the end-member values of stable nitrogen isotopes for accurately characterizing emission sources using nitrogen. This study provides valuable insights into the relationship between emission sources and oxidative potentials (OP), emphasizing the increased contribution of coal combustion during the cold season and non-fossil sources during the warm season to the elevated OP of $PM_{2.5}$.

3.5. $PM_{2.5}$ mass normalized oxidative potential

In evaluating the overall dependence of DTTv on $PM_{2.5}$ mass, DTTv was normalized by $PM_{2.5}$ concentration (DTTm) and subsequently, DTTm was correlated with the relative abundance of major constituents to $PM_{2.5}$ concentrations (Fig. 7). The results clearly indicate that the oxidative potential per unit mass was highest at the lowest $PM_{2.5}$ concentrations, coinciding with a reduced contribution of secondary inorganic ions to $PM_{2.5}$. In contrast, the ratios of WSOC/$PM_{2.5}$ and EC/$PM_{2.5}$ were notably elevated at the highest DTTm ranges. A notable observation is that the highest range of DTTv values was associated with the highest concentrations of secondary inorganic ions whose mass fraction within $PM_{2.5}$ was substantially higher compared to that of EC or WSOC (Fig. 2). In addition to EC and WSOC, the concentrations of heavy metals such as V, Ni, and Fe were found to be elevated in the highest DTTm range (not shown), although lacking a strong correlation with DTTv. As discussed earlier, these species indicate the local influence from vehicle emissions during the warm season. These findings capture the seasonal variability of $PM_{2.5}$ in the study region and underscores that under low $PM_{2.5}$ conditions, liquid fossil fuels from vehicle emissions are likely to play a crucial role in affecting OP. Therefore, it can be suggested that the reduction of emissions from even less dominant local sources is significant in terms of oxidative potential, especially when $PM_{2.5}$ concentrations are low.

4. Conclusion

The findings of this study estimate more intuitive sources of emissions that contribute oxidative potential (OP) through the analysis of carbon and nitrogen isotopes in $PM_{2.5}$ collected in the megacity, Seoul. Oxidative potential, as measured by the DTT assay, demonstrated significant correlations with the mass concentration of $PM_{2.5}$ and its key components, including inorganic nitrogen and organic carbon. These results, in conjunction with geographical sources identified through $PM_{2.5}$ measurements and air mass trajectory calculations, suggest an increased contribution from fossil fuel, especially coal combustion, during the cold season when intensified northwesterly winds effectively transported outflows from the Asian continent. It is noteworthy that, although the contribution of EC and WSOC to $PM_{2.5}$ mass was generally less prominent than those of secondary inorganic ions, their relative abundance was significantly elevated at the highest DTTv per mass (DTTm). In warm seasons, the influence of liquid fossil fuel, mainly from vehicle emissions, became more pronounced, which likely to contributed to the formation of nitrogen-containing organic carbon and impacted oxidative potential. These findings emphasize the importance of reducing vehicle exhaust emission in relation to the oxidative potential of $PM_{2.5}$, and provide insights for developing targeted emission control strategies in urban environments, ultimately contributing to improved air quality and public health protection.

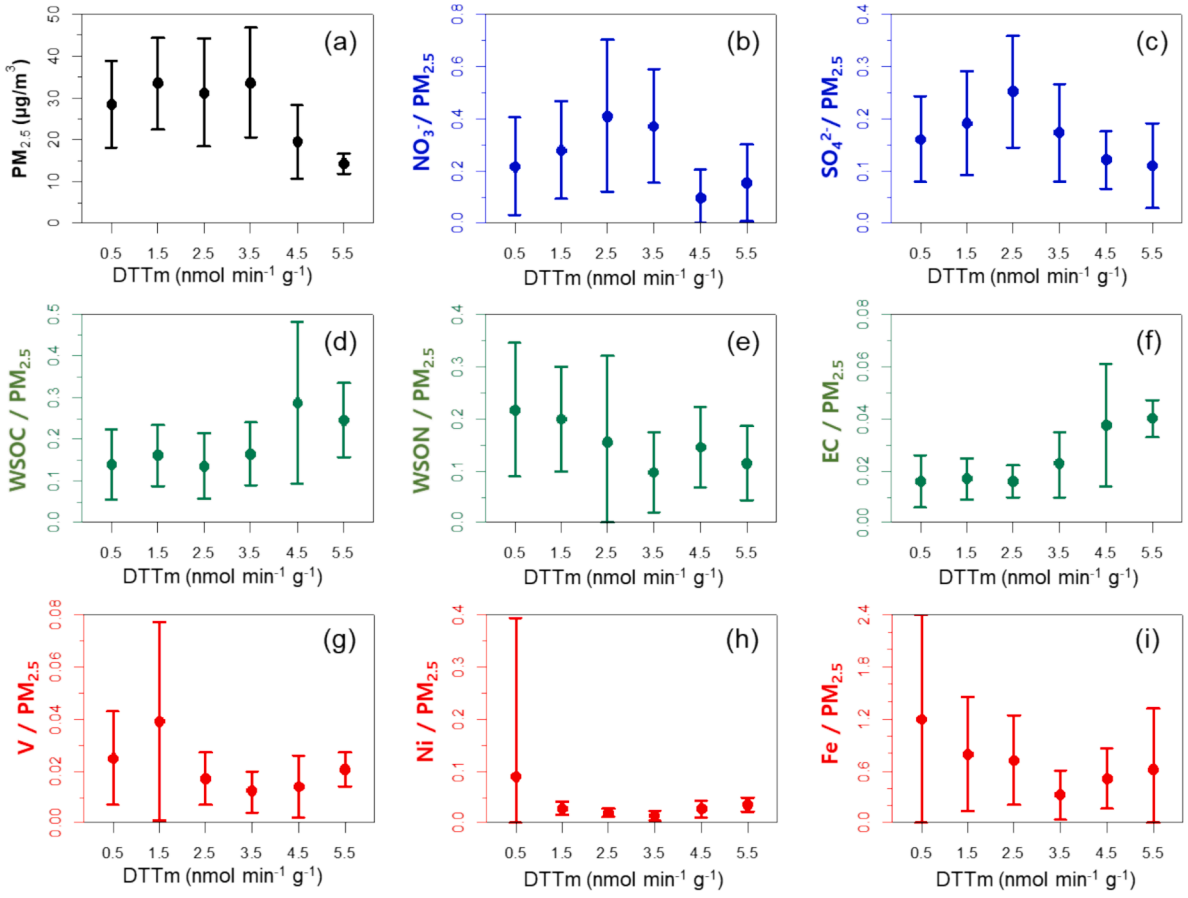

Fig. 7. Ratio of each chemical component to $PM_{2.5}$ mass in mass normalized DTT activities. A value between 0 and 1 is indicated as 0.5, a value between 1 and 2 is indicated as 1.5, and the average and standard deviation (σ) are displayed for each DTTm level.

CRediT authorship contribution statement

Joo-Ae Kim: Writing – original draft, Visualization, Validation, Investigation, Formal analysis, Data curation, Conceptualization. **Seulki Jeong:** Writing – original draft, Visualization, Validation, Investigation, Formal analysis, Data curation, Conceptualization. **Saehee Lim:** Resources, Data curation. **Yongjoo Choi:** Resources, Data curation. **Hyomin Kim:** Methodology, Investigation, Data curation. **Meehye Lee:** Writing – review & editing, Supervision, Resources, Project administration, Conceptualization.

Declaration of competing interest

The authors declare that they have no known competing financial interests or personal relationships that could have appeared to influence the work reported in this paper.

Acknowledgements

This work was supported by the Korea Basic Science Institute (KBSI) projects (C180200 and C280200) and funded by the Korea Institute of Science and Technology (KIST) through grant 2E32360-23-P007. And Seulki Jeong thanks for Korea Institute of Marine Science & Technology Promotion (KIMST) funded by the Ministry of Oceans and Fisheries (RS-2023-00254680).

Data availability

Data will be made available on request.

References

Agnihotri, R., Mandal, T., Karapurkar, S., Naja, M., Gadi, R., Ahammmed, Y.N., Kumar, A., Saud, T., Saxena, M., 2011. Stable carbon and nitrogen isotopic composition of bulk aerosols over India and northern Indian Ocean. Atmos. Environ. 45 (17), 2828–2835. https://doi.org/10.1016/j.atmosenv.2011.03.003.

Ancelet, T., Davy, P.K., Trompetter, W.J., Markwitz, A., Weatherburn, D.C., 2011. Carbonaceous aerosols in an urban tunnel. Atmos. Environ. 45 (26), 4463–4469. https://doi.org/10.1016/j.atmosenv.2011.05.032.

Ayres, J.G., Borm, P., Cassee, F.R., Castranova, V., Donaldson, K., Ghio, A., Harrison, R. M., Hider, R., Kelly, F., Kooter, I.M., 2008. Evaluating the toxicity of airborne particulate matter and nanoparticles by measuring oxidative stress potential—a workshop report and consensus statement. Inhal. Toxicol. 20 (1), 75–99. https://doi.org/10.1080/08958370701665517.

Bae, M., Schauer, J., Lee, T., Jeong, J., Kim, Y., Ro, C., Song, S., Shon, Z., 2017. Relationship between reactive oxygen species and water-soluble organic compounds: Time-resolved benzene carboxylic acids measurement in the coastal area during the KORUS-AQ campaign. Environ. Pollut. 231 (1), 1–12. https://doi.org/10.1016/j.envpol.2017.07.100. Epub 2017 Aug 1 PMID: 28777977.

Bates, J.T., Weber, R.J., Abrams, J., Verma, V., Fang, T., Klein, M., Strickland, M.J., Sarnat, S.E., Chang, H.H., Mulholland, J.A., 2015. Reactive oxygen species generation linked to sources of atmospheric particulate matter and cardiorespiratory effects. Environ. Sci. Tech. 49 (22), 13605–13612. https://doi.org/10.1021/acs.est.5b02967.

Bird, M.I., Ascough, P.L., 2012. Isotopes in pyrogenic carbon: a review. Org. Geochem. 42 (12), 1529–1539. https://doi.org/10.1016/j.orggeochem.2010.09.005.

Charrier, J.G., Anastasio, C., 2011. Impacts of antioxidants on hydroxyl radical production from individual and mixed transition metals in a surrogate lung fluid. Atmos. Environ. 45 (40), 7555–7562. https://doi.org/10.1016/j.atmosenv.2010.12.021.

Charrier, J.G., Anastasio, C., 2012. On dithiothreitol (DTT) as a measure of oxidative potential for ambient particles: evidence for the importance of soluble transition metals. Atmos. Chem. Phys. (print) 12 (5), 11317. https://doi.org/10.5194/acpd-12-11317-2012.

Chen, Q., Wang, M., Wang, Y., Zhang, L., Li, Y., Han, Y., 2019. Oxidative potential of water-soluble matter associated with chromophoric substances in PM2. 5 over Xi'an. China. Environ. Sci. Technol. 53 (15), 8574–8584. https://doi.org/10.1021/acs.est.9b01976.

Chen, Y.-J., Cai, W.-W., Huang, G.-P., Li, J., Zhang, G., 2012. Stable carbon isotope of black carbon from typical emission sources in China. Huan Jing ke Xue=. Huanjing Kexue 33 (3), 673–678.

Cheng, Y., Engling, G., He, K.-B., Duan, F.-K., Ma, Y.-L., Du, Z.-Y., Liu, J.-M., Zheng, M., Weber, R.J., 2013. Biomass burning contribution to Beijing aerosol. Atmos. Chem. Phys. 13 (15), 7765–7781. https://doi.org/10.5194/acp-13-7765-2013.

Cheng, Y., Ma, Y., Dong, B., Qiu, X., Hu, D., 2021. Pollutants from primary sources dominate the oxidative potential of water-soluble PM2. 5 in Hong Kong in terms of dithiothreitol (DTT) consumption and hydroxyl radical production. J. Hazard. Mater. 405, 124218. https://doi.org/10.1016/j.jhazmat.2020.124218.

Cho, A.K., Sioutas, C., Miguel, A.H., Kumagai, Y., Schmitz, D.A., Singh, M., Eiguren-Fernandez, A., Froines, J.R., 2005. Redox activity of airborne particulate matter at different sites in the Los Angeles Basin. Environ. Res. 99 (1), 40–47. https://doi.org/10.1016/j.envres.2005.01.003.

Dai, Q., Liu, B., Bi, X., Wu, J., Liang, D., Zhang, Y., Feng, Y., Hopke, P.K., 2020. Dispersion normalized PMF provides insights into the significant changes in source contributions to PM2. 5 after the COVID-19 outbreak. Environ. Sci. Tech. 54 (16), 9917–9927. https://doi.org/10.1021/acs.est.0c02776.

Ding, A., Huang, X., Nie, W., Chi, X., Xu, Z., Zheng, L., Xu, Z., Xie, Y., Qi, X., Shen, Y., 2019. Significant reduction of PM 2.5 in eastern China due to regional-scale emission control: evidence from SORPES in 2011–2018. Atmos. Chem. Phys. 19 (18), 11791–11801. https://doi.org/10.5194/acp-19-11791-2019.

Draxler, R., Stunder, B., Rolph, G., Stein, A., & Taylor, A. (2016). HYSPLIT4 User's Guide Version 4-Last Revision: February 2016. HYSPLIT Air Resources Laboratory: College Park, MD, USA.

Fajersztajn, L., Veras, M., Barrozo, L.V., Saldiva, P., 2013. Air pollution: a potentially modifiable risk factor for lung cancer. Nat. Rev. Cancer 13 (9), 674–678. https://doi.org/10.1038/nrc3572.

Fang, T., Verma, V., Bates, J.T., Abrams, J., Klein, M., Strickland, M.J., Sarnat, S.E., Chang, H.H., Mulholland, J.A., Tolbert, P.E., 2016. Oxidative potential of ambient water-soluble PM 2.5 in the southeastern United States: contrasts in sources and health associations between ascorbic acid (AA) and dithiothreitol (DTT) assays. Atmos. Chem. Phys. 16 (6), 3865–3879. https://doi.org/10.5194/acp-16-3865-2016.

Gao, D., Godri Pollitt, K.J., Mulholland, J.A., Russell, A.G., Weber, R.J., 2020. Characterization and comparison of PM 2.5 oxidative potential assessed by two acellular assays. Atmos. Chem. Phys. 20 (9), 5197–5210. https://doi.org/10.5194/acp-20-5197-2020.

Gil, J., Lee, M., Lee, H., Jang, J., 2023. Seasonal Characteristics of HONO Variations in Seoul during 2021–2022. J. Korean Soc. Atmos. Environ. 39 (3), 308–319. https://doi.org/10.5572/KOSAE.2023.39.3.308.

Gleason, J.D., Kyser, T.K., 1984. Stable isotope compositions of gases and vegetation near naturally burning coal. Nature 307 (5948), 254–257. https://doi.org/10.1038/307254a0.

Glojek, K., Thuy, D.N.V., Weber, S., Uzu, G., Manousakas, M., Elazzouzi, R., Džepina, K., Darfeuil, S., Ginot, P., Jaffrezo, J.L., Žabkar, R., Turšič, J., Podkoritnik, A., Močnik, M., 2024. Annual variation of source contributions to PM10 and oxidative potential in a mountainous area with traffic, biomass burning, cement-plant and biogenic influences. Environ. Int. 189. https://doi.org/10.1016/j.envint.2024.108787.

Ham, J., Suh, I., Lee, M., Kim, H., Kim, S., 2021. Elemental carbon observed at a peri-urban forest site near the seoul metropolitan area as a tracer of seasonal haze occurrence. Atmos. 12 (12), 1627. https://doi.org/10.3390/atmos12121627.

Hsu, Y., Holsen, T.M., Hopke, P.K., 2003. Comparison of hybrid receptor models to locate PCB sources in Chicago. Atmos. Environ. 37, 545–562. https://doi.org/10.1016/S1352-2310(02)00886-5.

Jo, H.-Y., Lee, H.-J., Jo, Y.-J., Heo, G., Lee, M., Kim, J.-A., Park, M.-S., Lee, T., Kim, S.-W., Lee, Y.-H., 2022. A case study of heavy PM2. 5 secondary formation by N2O5 nocturnal chemistry in Seoul, Korea in January 2018: Model performance and error analysis. Atmos. Res. 266, 105951. https://doi.org/10.1016/j.atmosres.2021.105951.

Joo, T., Rogers, M.J., Soong, C., Hass-Mitchell, T., Heo, S., Bell, M.L., Ng, N.L., Gentner, D.R., 2024. Aged and obscured wildfire smoke associated with downwind health risks. Environ. Sci. Technol. Lett. 11 (12), 1340–1347. https://doi.org/10.1021/acs.estlett.4c00785.

Kajino, M., Hagino, H., Fujitani, Y., Morikawa, T., Fukui, T., Onishi, K., Okuda, T., Igarashi, Y., 2021. Simulation of the transition metal-based cumulative oxidative potential in East Asia and its emission sources in Japan. Sci. Rep. 11 (1), 6550. https://doi.org/10.1038/s41598-021-85894-z.

Kang, S., Choi, S., Ban, J., Kim, K., Singh, R., Park, G., Kim, M.-B., Yu, D.-G., Kim, J.-A., Kim, S.-W., 2022. Chemical characteristics and sources of PM2. 5 in the urban environment of Seoul, Korea. Atmos. Pollut. Res. 13 (11), 101568. https://doi.org/10.1016/j.apr.2022.101568.

Kawashima, H., Haneishi, Y., 2012. Effects of combustion emissions from the Eurasian continent in winter on seasonal δ_{13}C of elemental carbon in aerosols in Japan. Atmos. Environ. 46, 568–579. https://doi.org/10.1016/j.atmosenv.2011.05.015.

Kim, H., Gil, J., Lee, M., Jung, J., Whitehill, A., Szykman, J., Lee, G., Kim, D.-S., Cho, S., Ahn, J.-Y., 2020a. Factors controlling surface ozone in the Seoul Metropolitan Area during the KORUS-AQ campaign. Elem. Sci. Anth. 8, 46. https://doi.org/10.1525/elementa.444.

Kim, J.-A., Lim, S., Shang, X., Lee, M., Kang, K.-S., Ghim, Y.S., 2020b. Characteristics of PM2. 5 chemical composition and high-concentration Episodes observed in Jeju. J. Korean Soc. Atmos. Environ. 36 (3). https://doi.org/10.5572/KOSAE.2020.36.3.388 from 2013 to 2016.

Kim, N.-K., Kim, Y.-P., Shin, H.-J., Lee, J.-Y., 2022. Long-term trend of the levels of ambient air pollutants of a megacity and a background area in Korea. Appl. Sci. 12 (8), 4039. https://doi.org/10.3390/app12084039.

Lang, J., Zhang, Y., Zhou, Y., Cheng, S., Chen, D., Guo, X., Chen, S., Li, X., Xing, X., Wang, H., 2017. Trends of PM2. 5 and chemical composition in Beijing, 2000-2015. Aerosol Air Qual. Res. 17 (2), 412–425. https://doi.org/10.4209/aaqr.2016.07.0307.

Lee, T., Go, S., Lee, Y.G., Park, S.S., Park, J., Koo, J.-H., 2022. Temporal variability of surface air pollutants in megacities of South Korea. Front. Environ. Sci. 10, 915531. https://doi.org/10.3389/fenvs.2022.915531.

Li, X., Kuang, X.M., Yan, C., Ma, S., Paulson, S.E., Zhu, T., Zhang, Y., Zheng, M., 2018. Oxidative potential by PM2.5 in the North China Plain: generation of hydroxyl radical. Environ. Sci. Tech. 53 (1), 512–520. https://doi.org/10.1021/acs.est.8b05253.

Li, Z., Nie, D., Chen, M., Ge, P., Liu, Z., Ma, X., Ge, X., Gu, R., 2021. Seasonal variation of oxidative potential of water-soluble components in $PM_{2.5}$ and PM_1 in the Yangtze River Delta. China. Air Qual Atmos Health 14, 1825–1836. https://doi.org/10.1007/s11869-021-01056-0.

Liang, L., Engling, G., Liu, C., Xu, W., Liu, X., Cheng, Y., Du, Z., Zhang, G., Sun, J., Zhang, X., 2021. Measurement report: Chemical characteristics of PM 2.5 during typical biomass burning season at an agricultural site of the North China Plain. Atmos. Chem. Phys. 21 (4), 3181–3192. https://doi.org/10.5194/acp-21-3181-2021.

Lim, S., Yang, X., Lee, M., Li, G., Gao, Y., Shang, X., Zhang, K., Czimczik, C.I., Xu, X., Bae, M.-S., 2020. Fossil-driven secondary inorganic $PM_{2.5}$ enhancement in the North China Plain: evidence from carbon and nitrogen isotopes. Environ. Pollut. 266, 115163. https://doi.org/10.1016/j.envpol.2020.115163.

Lim, S., Hwang, J., Lee, M., Czimczik, C.I., Xu, X., Savarino, J., 2022. Robust evidence of 14C, 13C, and 15N analyses indicating fossil fuel sources for total carbon and ammonium in fine aerosols in Seoul Megacity. Environ. Sci. Tech. 56 (11), 6894–6904. https://doi.org/10.1021/acs.est.1c03903.

Lim, S., Lee, M., Yoo, H.-J., 2023. Size distributions, mixing state, and morphology of refractory black carbon in an urban atmosphere of northeast Asia during summer. Sci. Total Environ. 856, 158436. https://doi.org/10.1016/j.scitotenv.2022.158436.

Lin, P., Yu, J.Z., 2011. Generation of reactive oxygen species mediated by humic-like substances in atmospheric aerosols. Environ. Sci. Tech. 45 (24), 10362–10368. https://doi.org/10.1021/es2028229.

Liu, F., Joo, T., Ditto, J.C., Saavedra, M.G., Takeuchi, M., Boris, A.J., Yang, Y., Weber, R. J., Dillner, A.M., Gentner, D.R., Ng, N.L., 2023. Oxidized and unsaturated: key organic aerosol traits associated with cellular reactive oxygen species production in the Southeastern United States. Environ. Sci. Technol 57 (38), 14150–14161. https://doi.org/10.1021/acs.est.3c03641.

Lovett, C., Sowlat, M.H., Saliba, N.A., Shihadeh, A.L., Sioutas, C., 2018. Oxidative potential of ambient particulate matter in Beirut during Saharan and Arabian dust events. Atmos. Environ. 188, 34–42. https://doi.org/10.1016/j.atmosenv.2018.06.016.

Miyazaki, K., Sekiya, T., Fu, D., Bowman, K., Kulawik, S., Sudo, K., Walker, T., Kanaya, Y., Takigawa, M., Ogochi, K., 2019. Balance of emission and dynamical controls on ozone during the Korea-United States Air Quality campaign from multiconstituent satellite data assimilation. J. Geophys. Res. Atmos. 124 (1), 387–413. https://doi.org/10.1029/2018JD028912.

Pachon, J.E., Weber, R.J., Zhang, X., Mulholland, J.A., Russell, A.G., 2013. Revising the use of potassium (K) in the source apportionment of PM2. 5. Atmos. Pollut. Res. 4 (1), 14–21. https://doi.org/10.5094/APR.2013.002.

Park, J., Park, E.H., Schauer, J.J., Yi, S.-M., Heo, J., 2018. Reactive oxygen species (ROS) activity of ambient fine particles (PM2. 5) measured in Seoul. Korea. Environ. Int. 117, 276–283. https://doi.org/10.1016/j.envint.2018.05.018.

Pascal, L., Pascal, M., Stempfelet, M., Goria, S., Declercq, C., 2013. Ecological study on hospitalizations for cancer, cardiovascular, and respiratory diseases in the industrial area of Etang-de-Berre in the South of France. J. Environ. Public Health 2013. https://doi.org/10.1155/2013/328737.

Patel, A., Rastogi, N., Rangu, S., Dave, J., Borgohain, A., Kundu, S.S., 2022. Oxidative potential and hydroxyl radical generation capacity of ambient PM2. 5 over a high-altitude site in northeastern Himalaya: Role of long-range transport. Atmos. Environ. 287, 119263. https://doi.org/10.1016/j.atmosenv.2022.119263.

Peters, A., Veronesi, B., Calderón-Garcidueñas, L., Gehr, P., Chen, L.C., Geiser, M., Reed, W., Rothen-Rutishauser, B., Schürch, S., Schulz, H., 2006. Translocation and potential neurological effects of fine and ultrafine particles a critical update. Part. Fibre Toxicol. 3 (1), 1–13. https://doi.org/10.1186/1743-8977-3-13.

Peterson, D.A., Hyer, E.J., Han, S.-O., Crawford, J.H., Park, R.J., Holz, R., Kuehn, R.E., Eloranta, E., Knote, C., Jordan, C.E., 2019. Meteorology influencing springtime air quality, pollution transport, and visibility in Korea. Elem. Sci. Anth. 7, 57. https://doi.org/10.1525/elementa.395.

Pizzino, G., Irrera, N., Cucinotta, M., Pallio, G., Mannino, F., Arcoraci, V., Squadrito, F., Altavilla, D., Bitto, A., 2017. Oxidative stress: harms and benefits for human health. Oxid. Med. Cell. Longev. 2017. https://doi.org/10.1155/2017/8416763.

Savic, A., Gil, J., Cha, J., Lee, M., Choi, Y., Park, M., 2024. Exploring the long-term variations and high concentration episodes of peroxyacetyl nitrate in Megacity Seoul. Atmos. Environ. 338, 120821. https://doi.org/10.1016/j.atmosenv.2024.120821.

Sint, T., Donohue, J.F., Ghio, A.J., 2008. Ambient air pollution particles and the acute exacerbation of chronic obstructive pulmonary disease. Inhal. Toxicol. 20 (1), 25–29. https://doi.org/10.1080/08958370701758759.

Srivastava, D., Xu, J., Vu, T.V., Liu, D., Li, L., Fu, P., Hou, S., Moreno Palmerola, N., Shi, Z., Harrison, R.M., 2021. Insight into PM 2.5 sources by applying positive matrix factorization (PMF) at urban and rural sites of Beijing. Atmos. Chem. Phys. 21 (19), 14703–14724. https://doi.org/10.5194/acp-21-14703-2021.

Tang, G., 2001. δ13C Characteristics of Carboniferous Coal in North China and Its Paleo Geographic Implications, (Political Scholars Anthology of Peking University). Peking University, Beijing.

Tanner, R.L., Miguel, A.H., 1989. Carbonaceous aerosol sources in Rio de Janeiro. Aerosol Sci. Tech. 10 (1), 213–223. https://doi.org/10.1080/02786828908959236.

Verma, V., Ning, Z., Cho, A.K., Schauer, J.J., Shafer, M.M., Sioutas, C., 2009. Redox activity of urban quasi-ultrafine particles from primary and secondary sources. Atmos. Environ. 43 (40), 6360–6368. https://doi.org/10.1016/j.atmosenv.2009.09.019.

Verma, V., Fang, T., Xu, L., Peltier, R.E., Russell, A.G., Ng, N.L., Weber, R.J., 2015a. Organic aerosols associated with the generation of reactive oxygen species (ROS) by water-soluble PM2.5. Environ. Sci. Tech. 49 (7), 4646–4656. https://doi.org/10.1021/es505577w.

Verma, V., Wang, Y., El-Afifi, R., Fang, T., Rowland, J., Russell, A.G., Weber, R.J., 2015b. Fractionating ambient humic-like substances (HULIS) for their reactive oxygen species activity–Assessing the importance of quinones and atmospheric aging. Atmos. Environ. 120, 351–359. https://doi.org/10.1016/j.atmosenv.2015.09.010.

Wang, J., Lin, X., Lu, L., Wu, Y., Zhang, H., Lv, Q., Liu, W., Zhang, Y., Zhuang, S., 2019. Temporal variation of oxidative potential of water soluble components of ambient PM2. 5 measured by dithiothreitol (DTT) assay. Sci. Total Environ. 649, 969–978. https://doi.org/10.1016/j.scitotenv.2018.08.375.

Wang, W., Zhang, Y., Cao, G., Song, Y., Zhang, J., Li, R., Zhao, L., Dong, C., Cai, Z., 2022. Influence of COVID-19 lockdown on the variation of organic aerosols: Insight into its molecular composition and oxidative potential. Environ. Res. 206, 112597. https://doi.org/10.1016/j.envres.2021.112597.

Wang, X., Bi, X., Li, H., Zhang, W., Dai, Q., Song, L., Li, L., Wu, J., Zhang, Y., Feng, Y., 2023. The role of sources and meteorology in driving PM2. 5-bound chlorine. J. Hazard. Mater. 441, 129910. https://doi.org/10.1016/j.jhazmat.2022.129910.

Widory, D., 2006. Combustibles, fuels and their combustion products: a view through carbon isotopes. Combust. Theor. Model. 10 (5), 831–841. https://doi.org/10.1080/13647830600720264.

Win, M.S., Tian, Z., Zhao, H., Xiao, K., Peng, J., Shang, Y., Wu, M., Xiu, G., Lu, S., Yonemochi, S., 2018. Atmospheric HULIS and its ability to mediate the reactive oxygen species (ROS): A review. J. Environ. Sci. 71, 13–31. https://doi.org/10.1016/j.jes.2017.12.004.

World Health Organization (WHO) (2020) The top 10 causes of death, https://www.who.int/news-room/fact-sheets/detail/the-top-10-causes-of-death.

Xiong, Q., Yu, H., Wang, R., Wei, J., Verma, V., 2017. Rethinking dithiothreitol-based particulate matter oxidative potential: measuring dithiothreitol consumption versus reactive oxygen species generation. Environ. Sci. Tech. 51 (11), 6507–6514. https://doi.org/10.1021/acs.est.7b01272.

Xu, X., Trumbore, S.E., Zheng, S., Southon, J.R., McDuffee, K.E., Luttgen, M., Liu, J.C., 2007. Modifying a sealed tube zinc reduction method for preparation of AMS graphite targets: reducing background and attaining high precision. Nucl. Instrum. Methods Phys. Res., Sect. B 259 (1), 320–329. https://doi.org/10.1016/j.nimb.2007.01.175.

Yu, G.H., Park, S.S., Ghim, Y.S., Shin, H.J., Lim, C.S., Ban, S.J., Yu, J.A., Kang, H.J., Seo, Y.K., Kang, K.S., 2018. Difference in chemical composition of PM 2.5 and investigation of its causing factors between 2013 and 2015 in air pollution intensive monitoring stations. J. Korean Soc. Atmos. Environ. 34 (1), 16–37. https://doi.org/10.5572/KOSAE.2018.34.1.016.

Yu, S., Liu, W., Xu, Y., Yi, K., Zhou, M., Tao, S., Liu, W., 2019. Characteristics and oxidative potential of atmospheric PM2. 5 in Beijing: Source apportionment and seasonal variation. Sci. Total Environ. 650, 277–287. https://doi.org/10.1016/j.scitotenv.2018.09.021.

Yu, Y., Cheng, P., Li, Y., Gu, J., Gong, Y., Han, B., Yang, W., Sun, J., Wu, C., Song, W., 2022. The association of chemical composition particularly the heavy metals with the oxidative potential of ambient PM2. 5 in a megacity (Guangzhou) of southern China. Environ. Res. 213, 113489. https://doi.org/10.1016/j.envres.2022.113489.

Zhang, Q., Zheng, Y., Tong, D., Shao, M., Wang, S., Zhang, Y., Xu, X., Wang, J., He, H., Liu, W., 2019. Drivers of improved PM2. 5 air quality in China from 2013 to 2017. Proc. Natl. Acad. Sci. 116 (49), 24463–24469. https://doi.org/10.1073/pnas.1907956116.